AIP Journal of Applied Physics

Infrared spectroscopy of an epitaxial BaTiO3/SrTiO3 superlattice grown on a (110) SmScO3 substrate

V. Železný, A. Soukiassian, D. G. Schlom, and X. X. Xi

Citation: Journal of Applied Physics **115**, 184102 (2014); doi: 10.1063/1.4875877
View online: http://dx.doi.org/10.1063/1.4875877
View Table of Contents: http://scitation.aip.org/content/aip/journal/jap/115/18?ver=pdfcov
Published by the AIP Publishing

Infrared spectroscopy of an epitaxial $BaTiO_3/SrTiO_3$ superlattice grown on a (110) $SmScO_3$ substrate

V. Železný,[1,a)] A. Soukiassian,[2] D. G. Schlom,[2] and X. X. Xi[3]
[1]*Institute of Physics, ASCR, Na Slovance 2, 182 21 Prague 8, Czech Republic*
[2]*Department of Materials Science and Engineering, Cornell University, Ithaca, New York 14853-1501, USA and Kavli Institute at Cornell for Nanophase Materials Sciences, Ithaca, New York 14853, USA*
[3]*Department of Physics, Temple University, Philadelphia, Pennsylvania 19122, USA*

(Received 20 February 2014; accepted 29 April 2014; published online 9 May 2014)

Polarized infrared reflectance spectra of a $BaTiO_3/SrTiO_3$ superlattice deposited on the (110) cut of $SmScO_3$ substrate and bare substrate have been studied in the broad temperature range from 10 to 650 K. Strong infrared anisotropy of the $SmScO_3$ substrate was observed and explained as a projection of B_{1u} and $B_{2u}+B_{3u}$ phonons into the (110) plane. In the polarization parallel to the c-axis below 200 cm^{-1}, an anomaly in the temperature dependence of the spectra was observed. Fitting the superlattice and substrate spectra, the parameters of optical phonons and their temperature dependence were determined. The superlattice phonon frequencies show only classical behavior, it means frequency hardening on cooling. Anisotropy was also found in the superlattice phonon frequencies and their contributions to static permittivity. © *2014 AIP Publishing LLC*. [http://dx.doi.org/10.1063/1.4875877]

I. INTRODUCTION

Barium strontium titanate, $Ba_xSr_{1-x}TiO_3$ (BST), has been extensively studied for potential technical applications such as nonvolatile memories, tunable microwave devices, and microelectromechanical systems.[1] Its preparation in the form of thin films is even more profitable as it can be modified by doping or biaxial stress from substrates. These factors enhance its dielectric constant and polarization.[2,3] Ferroelectric superlattices offer another possibility to improve the ferroelectric film properties. The superlattices are systems whose physics is defined by ultrathin components and interfaces, having switchable polarization, ferroelectric Curie temperature, and dielectric and piezoelectric coefficients that can be tuned and optimized. The difference in the properties of thin films or superlattices compared with bulk materials has been a major issue of fundamental research especially the thickness scaling of their properties. The experimental results can be recently compared with the progress in first-principles calculation and numerical simulation methods.[4]

Ferroelectricity results from an instability of one polar lattice mode. Its frequency decreases on approaching the critical temperature and when reaches zero the phonon atomic displacement freezes in a ferroelectric phase. The order parameter of such phase transition is the static component of the eigenvector of the soft mode and it must be polar and of long wavelength. Its softening is connected by the Lyddane-Sachs-Teller relation with the divergence of the static dielectric constant at the Curie temperature.[5] Infrared spectroscopy is a very effective and nondestructive tool for studying and understanding lattice dynamics and the behavior of ferroelectrics. Analyzing infrared spectra one can obtain detailed information about optic phonons. It is an alternative and often complementary way to Raman scattering, which is very frequently used to study lattice dynamics.[6,7] It has different selection rules and can provide additional information about lattice vibrations. Incident infrared radiation directly couples to the polarization (order parameter), enabling one to extract the parameters of polar-phonon modes, including the ferroelectric soft mode. Varying temperature enables us to study nanoscale ferroelectric heterostructures in the vicinity of the phase transition. Until recently, however, the technique could not be effectively used for studies of superlattices because it was difficult to separate the signals coming from the superlattice and the substrate it was grown upon. This problem was partly overcome only a few years ago, when scandate single crystals, whose infrared spectra are quite distinct to those of the ferroelectric superlattices, were introduced as substrates. Ferroelectric superlattices have large permittivity, which can be caused by the conductivity of charged defects at layer interface.[8,9] In these cases, direct microwave and low-frequency dielectric measurements are difficult and infrared technique can be an useful tool to estimate their intrinsic permittivity.

In the present work, we performed infrared study of an epitaxial $BaTiO_3/SrTiO_3$ superlattice grown by MBE on a (110) $SmScO_3$ substrate. The temperature dependence of the in-plane polar phonons was studied with the aim to understand the lattice dynamics and particularly the soft mode behavior. Although there has been a number of Raman and infrared experiments on ceramic and thin film $Ba_xSr_{1-x}TiO_3$, there is practically no infrared work on ferroelectric superlattices. Special attention is paid to low-frequency (soft) phonons, which play essential role in structural phase transitions. Our results are compared with Raman study and the lattice dynamics is discussed in view of theoretical predictions.

a)Electronic mail: zelezny@fzu.cz

II. EXPERIMENTAL

The infrared reflectivity measurements were performed on fully commensurate $[(BaTiO_3)_8/(SrTiO_3)_4]_{40}$ superlattice fabricated from 8 and 4 unit-cell thick $BaTiO_3$ and $SrTiO_3$ layers, respectively, repeated 40 times along the growth direction.[10] They were deposited by reactive molecular-beam epitaxy on the (110) surface of $SmScO_3$ substrate using the non-standard setting *Pbnm* notation. The superlattice was grown by sequential shuttering of fluxes produced by constituent sublimation from low-temperature effusion cells. The superlattice structure was characterized by several techniques. High resolution transmission electron microscopy showed accurate periodicity and abrupt $BaTiO_3/SrTiO_3$ interfaces. X-ray diffraction confirmed excellent epitaxy and crystallinity. When $BaTiO_3$ ($a = 3.990$ Å) layers are combine with $SrTiO_3$ ($a = 3.905$ Å) layers in a superlattice, there is a relative large mismatch of 3% between their lattice parameters what induces strain in the superlattice itself. In the superlattice commensurate to $SmScO_3$ substrate at room temperature with effective in-plane lattice constant $a = 3.987$ Å, the $BaTiO_3$ layers are practically strain free having an out-of-plane polarization and the $SrTiO_3$ layers are under 2.2% tensional biaxial strain with an in-plane polarization. This implies that the interfaces between $SrTiO_3$ and $BaTiO_3$ are analogous to 90° domain walls, where the polarization turns from one direction to another one. The further details on the superlattice growth and its characterization can be found in Refs. 10 and 11.

Normal-incidence polarized infrared reflectance spectra were taken using a Fourier-transform spectrometer Bruker IFS 113v equipped with a He-cooled bolometer. The low-temperature measurements in the temperature range from 10 to 300 K were done using a continuous-flow Optistat CF cryostat with polyethylene windows which limited the spectral interval to 25–650 cm^{-1}. The high-temperature spectra from 300 to 650 K were measured in a furnace. Our room-temperature spectra were taken in a broader spectral range up to 3000 cm^{-1} which enabled us to determine the high-frequency contribution from electronic transitions included in ε_∞. The reflectance measurements were done independently for bare substrate and substrate covered with superlattice. Normal-incidence reflectance from bare substrate can be expressed as

$$R(\omega) = \left| \frac{\sqrt{\tilde{\varepsilon}(\omega)} - 1}{\sqrt{\tilde{\varepsilon}(\omega)} + 1} \right|^2, \quad (1)$$

where the complex dielectric function $\tilde{\varepsilon}(\omega)$ is calculated using the Drude-Lorentz formula, which describes the contributions of the modes laying in the plane of the sample surface as damped harmonic oscillators

$$\tilde{\varepsilon}(\omega) = \varepsilon_1(\omega) + i\varepsilon_2(\omega) = \varepsilon_\infty + \sum_{j=1}^{n} \frac{\Delta\varepsilon_j \omega_j^2}{\omega_j^2 - \omega^2 + i\omega\gamma_j}, \quad (2)$$

where ω_j is the transverse frequency of the jth polar mode, $\Delta\varepsilon_j$ its contribution to static permittivity, γ_j its damping constant, and high-frequency permittivity ε_∞ takes into account the contributions from higher energy optical transitions. The static permittivity is given by a sum of infrared-active phonons and electronic contributions

$$\varepsilon(0) = \varepsilon_\infty + \varepsilon_{ph} = \varepsilon_\infty + \sum_{j=1}^{n} \Delta\varepsilon_j. \quad (3)$$

More complicated expression for a multilayer system must be used to describe normal-incidence reflectance from a semi-infinite substrate covered by a superlattice. The reflectance is given in terms of complex Fresnel coefficients, which are related to the complex refractive indices of superlattice slab $\tilde{n}_f = n_f + ik_f$ and the substrate $\tilde{n}_s = n_s + ik_s$ and film thickness d. The details can be found in Refs. 12 and 13. The dielectric function for such superlattice cannot be modeled by the sum of all its modes, because their number in the superlattice with 12-unit cell period is too large ($47A_1 \oplus 12B_1 \oplus 59E$ for tetragonal phase).[14] Instead of it an effective medium model taking into account a hypothetical perovskite is used.

From the comparison of the lattice constants[11] and UV Raman data,[15] it follows that the $BaTiO_3$ layers in the superlattices grown on $SmScO_3$ are practically unstrained, while large tensile strain in the $SrTiO_3$ layers induces an in-plane polarization (orthorhombic phase). First-principles calculations[16] predict the spontaneous polarization along [001] and [110] in $SrTiO_3$ layers whereas, in $BaTiO_3$, only the polarization along [001] remains. The symmetry is lowered to monoclinic space group. The temperature evolution of Raman spectra shows a phase transition to the tetragonal phase,[15] which depends on the strain and the ratio of the $BaTiO_3$ and $SrTiO_3$ constituent layers. For our composition, T_C is found 660 K for fully strained superlattice and it drops almost to the bulk $BaTiO_3$ value for relaxed one.

III. RESULTS AND DISCUSSION

A. Infrared spectroscopy of the $SmScO_3$ substrate

Polarized infrared reflectance spectra of the $SmScO_3$ single crystalline substrate measured in both polarizations at various temperatures are shown in Figs. 1 and 2. The spectra from the (110) surface of substrate were measured with the infrared radiation polarized along the c axis and perpendicular to it. They show typical phonon reflection bands whose damping decreases on cooling and they become more pronounced and sharper. $SmScO_3$ has an orthorhombic structure with 4 molecules in primitive cell. Factor-group analysis in the Brillouin-zone center for the *Pbnm* (D_{2h}^{16}) distributes 25 infrared-active optic phonons among $7B_{1u} \oplus 9B_{2u} \oplus 9B_{3u}$ irreducible representations polarized along the crystal axes c, b, and a. On the (110) cut slab, this analysis predicts 7 infrared active modes along the c-axis and 18 perpendicular to it. The normal reflectance from the substrate was fitted with the model regarding the substrate as a semi-infinite medium and using the Drude-Lorentz formula given in Eqs. (1) and (2). Good fit was obtained by modeling the experimental spectra with 7 B_{1u} modes for the $E \parallel c$ polarization and 14 B_{2u} and B_{3u} modes for the $E \perp c$ polarization. The resulting fit phonon parameters are quoted in Table I. The complex dielectric

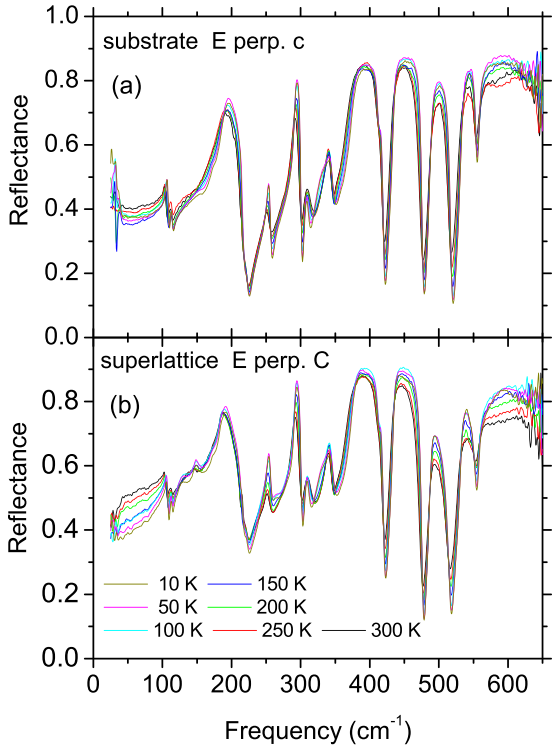

FIG. 1. Polarized reflectance of a bare $SmScO_3$ substrate (a) and superlattice (b) in the $E \perp c$ polarization at selected temperatures.

functions for both polarizations are given in Figs. 3 and 4. The number of the modes agrees with group analysis for the $E \parallel c$ polarization but the agreement is worse for the $E \perp c$ polarization, where 14 instead of expected 18 modes were found. This can be explained by the small oscillator strength

TABLE I. Phonon parameters obtained from the fits of the polarized reflectivity spectra of $SmScO_3$ substrate taken at 10 K ($\varepsilon_\infty = 4.5$).

	$E \parallel (001)$; B_{1u} mode			$E \perp (001)$; $B_{2u} + B_{3u}$ modes		
No.	ω_j (cm^{-1})	γ_j (cm^{-1})	$\Delta\varepsilon_j$	ω_j (cm^{-1})	γ_j (cm^{-1})	$\Delta\varepsilon_j$
1.	130.72	23.78	469.48	103.12	11.29	120.64
2.	155.69	10.32	51.31	113.14	2.31	31.43
3.	195.62	3.92	96.42	184.56	16.92	482.52
4.	305.79	10.27	495.36	219.03	1.82	12.52
5.	345.02	11.92	376.23	253.16	6.12	111.09
6.	378.47	12.05	526.45	290.34	5.58	339.20
7.	500.90	14. 93	365.96	310.89	14.94	260.52
8.				338.40	11.80	345.24
9.				369.29	12.82	669.63
10.				411.75	3.79	33.61
11.				430.98	8.03	335.13
12.				486.58	10.56	260.96
13.				527.00	10.81	255.22
14.				557.08	20.43	138.00

of the missing modes and overlapping of the B_{2u} and B_{3u} polarizations. Phonons in bulk earth scandates have been investigated using first-principles calculation[17] and their parameters are in good agreement with our experimental data. In the very low-frequency range below 50 cm^{-1} at low temperature, the substrate becomes partly transparent and the reflectivity increases due to multiple reflection from front and rear surfaces. This part of the spectra was not involved in our fit. Nevertheless, we found another mode in the polarization $E \parallel c$ at 40 cm^{-1}. Its nature is up to now unknown and it is probably electric origin.

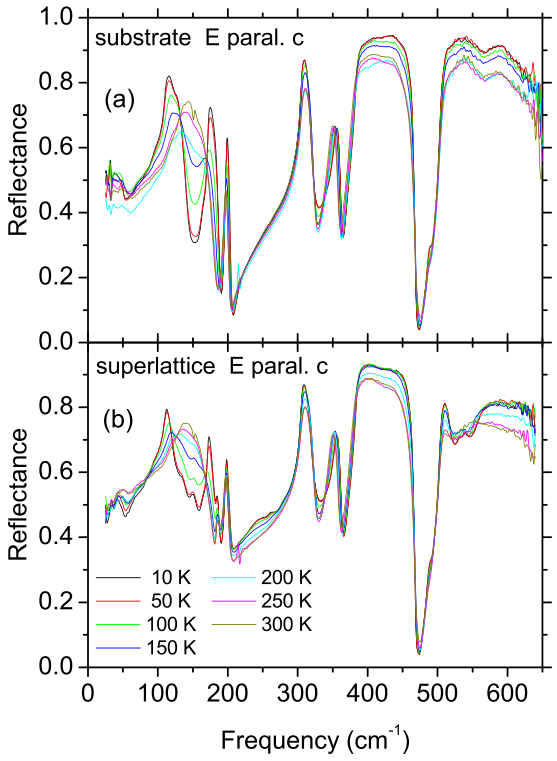

FIG. 2. Polarized reflectance of a bare $SmScO_3$ substrate (a) and superlattice (b) in the $E \parallel c$ polarization at selected temperatures.

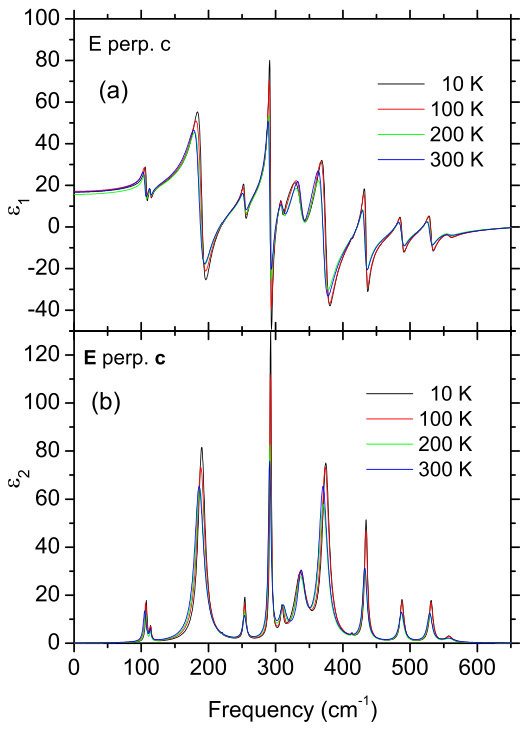

FIG. 3. Real and imaginary parts of the dielectric function of a bare $SmScO_3$ substrate in the $E \perp c$ polarization at selected temperatures.

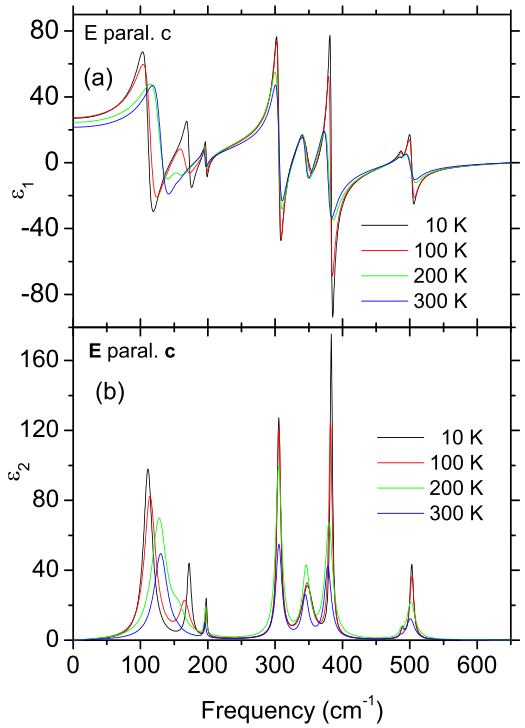

FIG. 4. Real and imaginary parts of the dielectric function of a bare $SmScO_3$ substrate and superlattice in the $E \parallel c$ polarization at selected temperatures.

The $SmScO_3$ substrate spectra show non-trivial and unusual temperature dependence in the frequency interval below 200 cm^{-1}, which is illustrated in Fig. 5. In the polarization of the electric field along the c-axis, the broad reflection band between 100 and 200 cm^{-1} starts to broaden on cooling and below 180 K splits into two bands, which draw apart on further cooling. Similar effect was observed also in other scandates.[18–20] It is not quite clear what is nature of this effect, because no structural changes in this temperature range are observed. The reflection in this spectral region is very strong and makes difficult to study infrared properties of any film or superlattice deposited on its top in this polarization. The conditions are much favorable in the polarization $E \perp c$, where only two weak bands are here present and the contribution of the superlattice plays more important role.

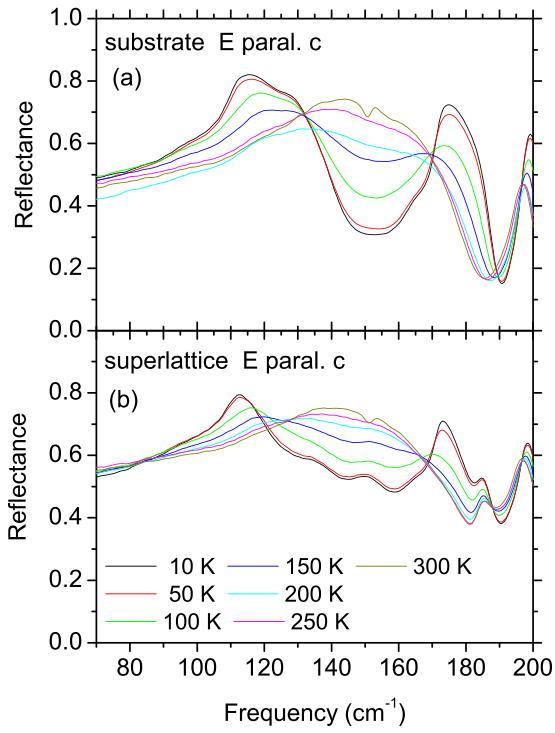

FIG. 5. Anomalous behavior of the reflectance of a bare $SmScO_3$ substrate and superlattice in the $E \parallel c$ polarization below 200 cm^{-1}.

B. Infrared spectroscopy of the $BaTiO_3/SrTiO_3$ superlattice

The vibrational properties of perovskites namely $BaTiO_3$ and $SrTiO_3$ have been extensively studied as a function of temperature by both Raman and infrared measurements and are well-known. In the paraelectric cubic phase of symmetry $Pm\bar{3}m\,(O_h^1)$, the 12 optic modes irreducibly transform as 3 $F_{1u}(\mathrm{IR}) + F_{2u}$. The F_{1u} modes known as TO_1, TO_2, and TO_4 are infrared active and the F_{2u} (TO_3) is the so-called silent mode. In the ferroelectric tetragonal phase of $P4\,mm$ (C_{4v}^1) symmetry, each of the F_{1u} triplet modes splits into A_1 (polarized along the tetragonal axis) and E (perpendicular to it) irreducible representations and the F_{2u} triplet splits into B_1 and E resulting in the 3 $A_1(\mathrm{IR,R}) + B_1(\mathrm{R}) + 4E(\mathrm{IR,R})$ irreducible decomposition. Here, IR and R stand for infrared and Raman modes activity, respectively. The polarized reflectance of the superlattice deposited on the top of $SmScO_3$ substrate is shown in Figs. 1(b) and 2(b). Most of the spectral features in both polarizations $E \perp c$ and $E \parallel c$ originate from $SmScO_3$ substrate. As the total thickness of the superlattice is only 192 nm, its role in the spectra is small but nevertheless differences between the spectra with and without the superlattice (comparing the panels (a) and (b) in Figs. 1 and 2) are clearly seen in the regions about 80, 180 and 500 cm^{-1} corresponding to the frequencies of TO_1, TO_2 and TO_4 perovskite modes, respectively. The spectra are measured at normal incidence and therefore only the phonons polarized in the sample plane can be observed. As the superlattice tetragonal axis is assumed in the direction of the superlattice growth, the three modes observed in the spectrum correspond to the E modes. No dramatic changes in the spectra are seen on varying temperature. The phonon damping classically decreases on cooling and therefore the intensity of the reflection bands increases. The frequencies of the lowest mode in the two polarizations ($E \perp c$ and $E \parallel c$) differ by 20 cm^{-1}. This can be explained by infrared anisotropy of the superlattice or substrate (deviations in lattice constants). It can also be caused by the difficulties in the determination of the phonon frequencies, which are due to the complex behavior of the $SmScO_3$ substrate in the polarization $E \parallel c$-axis. Interesting thing is their frequency variation on cooling. All three frequencies increase, whereas the lowest one by more than 50 cm^{-1}. The frequencies of two other modes are practically constant with temperature variation and no mode softening was observed in this superlattice on $SmScO_3$. This behavior of all three phonons shows that no phase transition can be expected in this temperature range.

Hence, it was interesting to explore the situation at high-temperature. The reflectance was measured from room

temperature up to 650 K. On heating, both polarizations show a decrease of reflectance bands and their further broadening due to increasing damping. There is also increase of noise in the spectra, which leads to that the extraction of the dielectric function is ambiguous. From the temperature development of reflectance, we can conclude that no phase transition can be indicated in this temperature range. This is little surprising because the Raman measurements showed the extinction of the scattered intensity of some peaks (TO_2 and TO_4), which connected to ferroelectric phase transition at 440 K[15] but these superlattices were grown on $DyScO_3$.

The structure and symmetry of $BaTiO_3/SrTiO_3$ superlattice are determined by strain due to in-plane lattice constant mismatch. This has been studied both theoretically[16,21] and experimentally.[22,23] The [110] polarization component is developed only in the $SrTiO_3$ layers and falls to zero in the $BaTiO_3$ layers, whereas the [001] polarization is approximately constant throughout the superlattice. With growing ratio Ba/Sr, the [001] component is larger and the [110] smaller. For our ratio of 2:1, the [001] component is dominating. Starting with these ideas, we can construct a model to interpret our experimental data.

In order to extract the phonon parameters of our superlattice from relatively complex reflectance spectrum, a fitting procedure was necessary to employ. For this purpose, we parametrized the dielectric function in the Drude-Lorentz form as given in Eq. (2). Using the two-layer model discussed above, we fixed all phonon parameters obtained from fit of the bare substrate. Then, a top superlattice layer was added to the model. Fitting procedure using the formula for coherence reflectance was similar to that used for superconducting systems.[24] Good agreement of calculated spectra with experimental enabled us to determine the effective parameters of the averaged superlattice consisting from $BaTiO_3$ and $SrTiO_3$ layers and calculate its response functions. The real and imaginary parts of the superlattice complex dielectric function are shown in Fig. 6 for the polarization $E \perp c$ and for the polarization $E \parallel c$ in Fig. 7. The superlattice spectrum was of a typical perovskite shape exhibiting three first-order peaks corresponding to TO_1, TO_2, and TO_4 polar phonons. Their positions coincide with the differences in the spectra of the superlattice and substrate mentioned in Figs. 1 and 2.

The superlattice deposited on the top of the substrate is oriented with the *c*-axis perpendicular to the substrate surface and its reflectance was measured in polarizations in the same directions as the substrate. The superlattice spectrum extracted from our experiment data represents a mixture of $SrTiO_3$ and $BaTiO_3$ spectra polarized perpendicular to the polar *c*-axis (*E*-symmetry). The spectrum can be interpreted as a mixture of its components in the ratio 1:2 and its form can be obtained in effective medium approximation. The temperature dependence of all three phonons is displayed in Fig. 8. The lowest frequency phonon is quite smeared; it is, therefore, very difficult to determine its parameters. Its frequency decreases on heating. This means that if there were any phase transition it would be above room temperature. The measurement at those temperatures did not show any indication of such behavior. This is in contradiction with

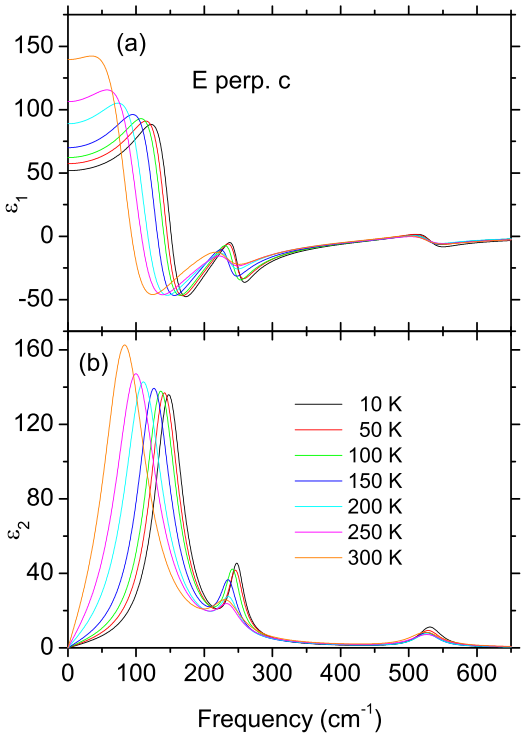

FIG. 6. Real and imaginary parts of the complex dielectric function of the superlattice in the $E \perp c$ polarization at selected temperatures.

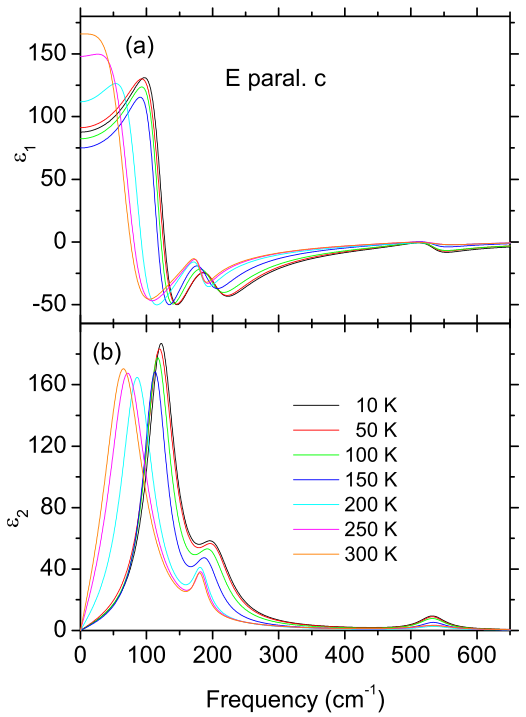

FIG. 7. Real and imaginary parts of the complex dielectric function of the superlattice in the $E \parallel c$ polarization at selected temperatures.

Raman measurement, but it was carried out on the superlattice grown on another substrate ($DyScO_3$).[15] In our case, we can say that we observe a classical behavior of the superlattice with hardening of its phonon modes on cooling. It is worth to note that in this respect the behavior of our superlattice was quite different from the very thin strained film

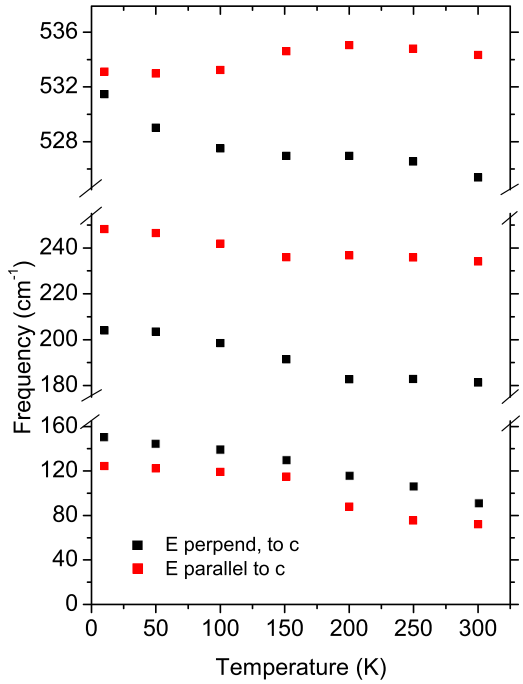

FIG. 8. Temperature dependence of the polar TO_1, TO_2, and TO_4 modes obtained from the fit of polarized reflectance of $BaTiO_3/SrTiO_3$ superlattice on $SmScO_3$ substrate.

(~10–20 nm), where the shift in the phase transition temperature was found.[18] This is probably due to large total thickness (192 nm) which results in its quenching in its own stable structure.

According to Eq. (3), the static dielectric tensor can be decomposed into a contribution ε_∞ arising from electronic response and the contribution from infrared-active phonon modes obtained by summing the contributions, $\Delta\varepsilon_j$, of all infrared-active modes,[25,26] which scale as $\tilde{Z}_j^{*2}/\omega_j^2$, where $\tilde{Z}_j^*$ is the scalar mode effective charge also proportional to plasma phonon frequency and ω_j is the eigenfrequency of the j mode. Looking at our modes temperature dependence it can be said that in the $E \parallel c$ polarization according to Eq. (3), $\varepsilon(0)$ varies from 90 at 10 K to 191.4 at 300 K and in the polarization $E \perp c$ from 55.4 at 10 K to 142.6 at 300 K. This behavior is consistent with the hardening of the phonons described above. The values for both polarizations are smaller than the values of both component materials in bulk form. This can be explained by smaller polarizability of our superlattice. Another interesting thing is the anisotropy the static permittivity, ε_0, which was also mentioned above.

IV. CONCLUSION

In summary, the polarized infrared reflectance of $(BaTiO_3)_8/(SrTiO_3)_4$ superlattices on (110) $SmScO_3$ substrate and bare substrate was measured in the temperature range 10 to 650 K. The dielectric functions and phonon parameters of the substrate were determined by fitting the reflectance spectra. The anisotropy in the spectra was explained in terms of B_{1u} and $(B_{2u} + B_{1u})$ phonon symmetries and their projection onto the (110) plane. An interesting anomaly was observed in the polarization $E \parallel c$ at temperature below 200 K, where a strong peak at 100 cm^{-1} split into two peaks separate by more than 50 cm^{-1} and some additional fine structure was found. The nature of this anomaly is up to now unknown but it probably comes from some electronic excitations. Similar features were also reported and interpreted in other compounds of this scandate family. Knowing the substrate data the phonon parameters and dielectric function of the superlattice were extracted using the thin-film substrate combination model and their temperature behavior was studied. The complex dielectric function of the superlattice can be modeled by an effective medium with three polar perovskite TO modes. In contrast to Raman scattering, we could observe the lowest-frequency mode on $(BaTiO_3)_8/(SrTiO_3)_4$ superlattices on scandate substrates. The mode TO_1, however, does not show any indication of soft mode behavior. In the whole temperature range, up to 650 K, its frequency is increasing with decreasing temperature. This can be explained that all our measurements were carried out at temperatures below T_C. As the phonon becomes smeared, the extraction of its parameters at higher temperature is not possible to determine. Another explanation of the low-frequency phonon behavior is that the superlattice is 192 nm thick and it quenches in its stable structure, which has no phase transition. If this is true it is not possible to learn by comparing our data with other experiments, because this is, to our knowledge, the first study of the dynamical properties of the superlattice on $SmScO_3$ substrate.

ACKNOWLEDGMENTS

This work was supported in part by the Grant Agency of the Czech Republic under Contract No. P204/11/1011.

[1]K. M. Rabe, C. H. Ahn, and J.-M. Triscone, *Physics of Ferroelectrics: A Modern Perspective* (Springer, 2007), Vol. 105.
[2]A. Erbil, Y. Kim, and R. A. Gerhardt, Phys. Rev. Lett. **77**, 1628 (1996).
[3]H. Tabata, H. Tanaka, and T. Kawai, Appl. Phys. Lett. **65**, 1970 (1994).
[4]D. G. Schlom, L.-Q. Chen, C. J. Fennie, V. Gopalan, D. A. Muller, X. Pan, R. Ramesh, and R. Uecker, MRS Bull. **39**, 118 (2014).
[5]D. A. Tenne and X. X. Xi, J. Am. Ceram. Soc. **91**, 1820 (2008).
[6]Y. I. Yuzyuk, R. S. Katiyar, V. A. Alyoshin, I. N. Zakharchenko, D. A. Markov, and E. V. Sviridov, Phys. Rev. B **68**, 104104 (2003).
[7]R. R. Das, Y. I. Yuzyuk, P. Bhattacharya, V. Gupta, and R. S. Katiyar, Phys. Rev. B **69**, 132302 (2004).
[8]D. O'Neill, R. M. Bowman, and J. M. Gregg, Appl. Phys. Lett. **77**, 1520 (2000).
[9]G. Catalan, D. O'Neill, R. M. Bowman, and J. M. Gregg, Appl. Phys. Lett. **77**, 3078 (2000).
[10]A. Soukiassian, W. Tian, V. Vaithyanathan, J. H. L. Chen, X. Xi, D. Schlom, D. Tenne, H. Sun, X. Pan, K. Choi *et al.*, J. Mater. Res. **23**, 1417 (2008).
[11]D. G. Schlom, L.-Q. Chen, C.-B. Eom, K. M. Rabe, S. K. Streiffer, and J.-M. Triscone, Annu. Rev. Mater. Res. **37**, 589 (2007).
[12]O. S. Heavens, *Optical Properties on Thin Solid Films* (Dover Publications, 1955).
[13]W. Vriens and W. Rippens, Appl. Opt. **22**, 4105 (1983).
[14]J. Hlinka, V. Železný, S. M. Nakhmanson, A. Soukiassian, X. X. Xi, and D. G. Schlom, Phys. Rev. B **82**, 224102 (2010).
[15]D. A. Tenne, A. Bruchhausen, N. D. Lanzillotti-Kimura, A. Fainstein, R. S. Katiyar, A. Cantarero, A. Soukiassian, V. Vaithyanathan, J. H. Haeni, W. Tian *et al.*, Science **313**, 1614 (2006).
[16]K. Johnston, X. Huang, J. B. Neaton, and K. M. Rabe, Phys. Rev. B **71**, 100103 (2005).
[17]S. Coh, T. Heeg, J. H. Haeni, M. D. Biegalski, J. Lettieri, L. F. Edge, K. E. O'Brien, M. Bernhagen, P. Reiche, R. Uecker *et al.*, Phys. Rev. B **82**, 064101 (2010).

[18]D. Nuzhnyy, J. Petzelt, S. Kamba, X. Martí, T. Čechal, C. M. Brooks, and D. G. Schlom, J. Phys. Condens. Matter **23**, 045901 (2011).
[19]S. Kamba, V. Goian, D. Nuzhnyy, V. Bovtun, M. Kempa, J. Prokleška, M. Bernhagen, R. Uecker, and D. G. Schlom, Phase Transitions **86**, 206 (2013).
[20]G. A. Komandin, E. S. Zhukova, V. I. Torgashev, A. V. Boris, A. A. Boris, E. A. Motovilova, A. S. Prokhorov, L. S. Kadyrov, B. P. Gorshunov, and M. Dressel, J. Appl. Phys. **114**, 024102 (2013).
[21]J. B. Neaton and K. M. Rabe, Appl. Phys. Lett. **82**, 1586 (2003).
[22]A. Q. Jiang, J. F. Scott, H. Lu, and Z. Chen, J. Appl. Phys. **93**, 1180 (2003).
[23]S. Ríos, A. Ruediger, A. Q. Jiang, J. F. Scott, H. Lu, and Z. Chen, J. Phys. Condens. Matter **15**, L305 (2003).
[24]P. Calvani, M. Capizzi, F. Donato, P. Dore, S. Lupi, P. Maselli, and C. Varsamis, Physica C **181**, 289 (1991).
[25]W. Zhong, R. D. King-Smith, and D. Vanderbilt, Phys. Rev. Lett. **72**, 3618 (1994).
[26]X. Gonze and C. Lee, Phys. Rev. B **55**, 10355 (1997).